American Mineralogist, Volume 87, pages 1215–1223, 2002

Ab initio quantum mechanical modeling of infrared vibrational frequencies of the OH group in dioctahedral phyllosilicates. Part I: Methods, results and comparison to experimental data

SARA MARTÍNEZ-ALONSO,[1,2,*] JAMES R. RUSTAD,[3] AND ALEXANDER F.H. GOETZ[1,2]

[1]Department of Geological Sciences, University of Colorado at Boulder, Boulder, Colorado 80309-0399, U.S.A.
[2]Center for the Study of Earth from Space, Cooperative Institute for Research in Environmental Sciences, Boulder, Colorado 80309-0216, U.S.A.
[3]W. R. Wiley Environmental Molecular Sciences Laboratory, Pacific Northwest National Laboratory, Richland, Washington 99352, U.S.A.

ABSTRACT

The infrared (IR) spectra of small clusters of atoms ($[MM'(OH)_2]$ and $[MM'(OH)_2(H_2O)_6]$, where M, M' = Al^{3+}, Mg^{2+}, Fe^{2+}, Fe^{3+}) mimicking the environment of the OH group in dioctahedral phyllosilicates have been modeled using ab initio quantum mechanical calculations. These modeling results are relevant to establishing the connections between IR spectra of phyllosilicates and their composition, and to investigate the utility of quantum mechanical models for calculating IR frequencies of minerals. This study focused on the OH stretch and in-plane bend fundamentals, because they give rise to a combination band near 4545 cm^{-1} (2.2 μm) that can be observed in imaging spectrometer or hyperspectral remote sensing data.

A comparison among results obtained using both ab initio [Hartree-Fock (HF) and Density Functional Theory (DFT)], and semi-empirical [PM3(tm)] methods, showed that the DFT model approaches IR frequency experimental values most closely.

IR spectra of phyllosilicates were modeled using the DFT method. The modeled frequencies were scaled using a mode-dependent linear transformation, and experimental frequencies were reproduced satisfactorily. The modeling results show that most of the variability observed in the OH in-plane bend fundamental of dioctahedral phyllosilicates can be explained by the effects of neighboring octahedral cations alone. Discrepancies between modeling and experimental results in the case of the OH stretch point to the existence of factors other than the nature of the neighboring octahedral cations, such as tetrahedral substitution, affecting this fundamental mode.

INTRODUCTION

IR spectroscopy of the OH group in phyllosilicates

The importance of spectroscopic studies of the OH fundamental modes of vibration for the understanding of crystalline structure and cationic composition of phyllosilicates was apparent very early on. Works by Tsuboi (1950), Sutherland (1955), Serratosa and Bradley (1958), Fripiat (1960), and Vedder and McDonald (1963) focused on the relationship between infrared (IR) spectra and crystalline structure of phyllosilicates, especially the OH orientation. Tuddenham and Lyon (1960) in natural samples, and Štubičan and Roy (1961) in synthetic minerals, observed gradual changes in the positions of certain IR absorption bands in the spectra of phyllosilicates with increasing cationic substitution. Jørgensen (1964) argued that such changes were distinct steps rather than gradual in nature.

In 1956 Beutelspacher correctly assigned the 925 cm^{-1} band as an octahedral cation-OH bending vibration. Vedder and McDonald (1963) refined that assignment, concluding that the 925 cm^{-1} band corresponded to the OH in-plane bend, δ(OH). These authors assigned the other two fundamentals involving OH in micas: 3628 cm^{-1} for the stretch, ν(OH), and 405 cm^{-1} for the out-of-plane OH bend, γ(OH). Vedder and McDonald (1963) also identified the combination of ν(OH) and δ(OH) occurring near 4542 cm^{-1} (2.2 μm). Unlike the OH fundamentals, the 2.2 μm combination band can be observed in reflected imaging spectrometer or hyperspectral remote sensing data, as it occurs in an atmospheric transmission window: a portion of the electromagnetic spectrum in which the absorption of incoming solar irradiance by atmospheric gases is minimal. Analysis of imaging spectrometer data can provide information on cationic composition of phyllosilicates and other minerals in large natural systems.

Numerous empirical studies showing correlation between the position of IR bands and composition of phyllosilicates followed (Farmer 1974 and references therein; King and Clark 1989; Clark et al. 1990; Post and Noble 1993; Duke 1994; Swayze 1997; Petit et al. 1999; Yang et al. 2001). Empirical observations indicate a correlation between the location of OH-related IR bands and cationic composition of the octahedral sheet in phyllosilicates, but not causation.

Modeling of the IR spectra of minerals

Quantum mechanical models (Head-Gordon 1996) apply the principles of quantum mechanics to calculating the static and dynamic properties of molecules. This is achieved through the analysis of the Born-Oppenheimer electronic Potential En-

* Present address: Laboratory for Atmospheric and Space Physics, University of Colorado, Boulder, CO 80309-0392, U.S.A. E-mail: martinas@lasp.colorado.edu

0003-004X/02/0809–1215$05.00

ergy Surface (PES) of the molecular system. For a molecule with n atoms, the PES is a $3n$-6 dimensional ($3n$-5 for linear molecules) hypersurface representing the energy of the system. The PES is calculated by approximately solving the Schrödinger equation. From the PES, various properties can be calculated, bond force constants among them. From bond force constants, frequencies of interatomic vibrations can be derived. Quantum mechanical models are considered ab initio if they do not incorporate any parameters fit experimentally, and semi-empirical otherwise.

The Hatree-Fock (HF) method (Hartree 1928a, 1928b; Fock 1930) is one of several ab initio methods utilized to solve the Schrödinger equation, based on finding an approximation to the exact wave function, a function of $3n$ variables, where n is the number of electrons in the system. The HF approximation does not include electron correlation effects. If these effects are incorporated into the model, it becomes extremely computing-intensive.

Density Functional Theory (DFT) is another ab initio method with a different approach to solving the Schrödinger equation, based on the fact that the total energy of an electron gas is a unique functional of the electron density (Hohenberg and Kohn 1964; Kohn and Sham 1965), that is, a function of only three variables. DFT methods account for electron correlation effects and are less computationally intensive than HF methods.

Semi-empirical calculations constitute a computationally faster, quantum mechanical approach. To account for the approximations made with these methods, empirically derived parameters are used. The accuracy of any semi-empirical method is limited to the accuracy of the experimental data used in obtaining the parameters (Stewart 1988).

Kubicki and co-workers (1993, 1995) carried out pioneering work on the prediction of IR spectra of minerals applying HF calculations to aluminosilicate molecules to investigate relationships between composition, structure, and IR vibrational fundamentals of OH. In their studies they explored the effect on the ν(OH) frequency of substitution of tetrahedral Si^{4+} by Al^{3+}. They also explored the effects of substitution of OH^- groups by H^- and F^-. Sainz-Díaz et al. (2000) extended the work done by Kubicki and co-workers by calculating ν(OH), δ(OH), and γ(OH) frequencies in an octahedral environment using the HF method. They included in their calculations cationic substitution of Al^{3+} by Mg^{2+} and Fe^{3+}.

In the present study, the IR spectra of small clusters of atoms mimicking the environment of the OH group in dioctahedral phyllosilicates have been modeled using DFT calculations and are compared to experimental data to test the hypothesis that the octahedral composition of phyllosilicates drives the variability observed in OH-related vibrations.

METHODOLOGY

Accuracy evaluation of the computational methods

To evaluate the accuracy of several computational methods available for the calculation of vibrational frequencies, quantum mechanical calculations for prototypical metal hydroxides in the gas phase were carried out and the results were compared with experimental frequencies. The results determined the computational method to be used when mimicking the environment of the OH group in dioctahedral phyllosilicates, and consequently the size of the clusters to be modeled.

HF calculations were performed using the software GAMESS (Schmidt et al. 1993). The program Cerius^2-DMol^3 (Accelrys, formerly Molecular Simulations Inc.) was utilized for DFT calculations. Semi-empirical calculations were performed with the software Spartan (Wavefunction, Inc.).

The following prototypical metal hydroxides were chosen because they include the cations that most commonly populate the octahedral sites in phyllosilicates: Al(OH), Mg(OH), and $Fe(OH)_2$. By studying these metal hydroxides, direct comparison between experimental and modeled frequencies on the same molecule was achieved.

Experimental data and modeling results derived from high-level HF ab initio calculations (which include electron correlation effects and very complete basis sets) for these three metal hydroxides in the gas phase were compiled from the literature (Hauge et al. 1980; Kauffman et al. 1985; Vacek et al. 1993; Pilgrim et al. 1993; Bunker et al. 1995; Kong and Boyd 1996). These data were compared to non-scaled wavenumbers calculated in this study for the same metal hydroxides at the HF/6-31G* (Hehre et al. 1972; Francl et al. 1982; Rassolov et al. 1998), HF/TZV (Dunning 1971; McLean and Chandler 1980; Rappe et al. 1981), DFT/DND (Becke 1988, 1993; Clark et al. 1983), and semi-empirical MNDO/PM3(tm) (Thiel and Voityuk 1992) levels of theory. The experimental values and modeling results for vibrational frequencies for the Al, Mg, and Fe^{2+} hydroxides are presented in Table 1.

This comparison shows that the DFT/DND method approximates experimental frequencies better than any of the other methods tested. This is in agreement with findings from Koch and Holthausen (2000). DFT accounting for electron correlation effects may be one of the reasons for the better performance of this method vs. HF, both when the latter uses the 6-31G* basis set and when it uses the more complete TZV basis set.

Wavenumbers calculated with the MNDO/PM3(tm) method show an erratic trend when compared with experimental values, making this method the less desirable for frequency calculation purposes. Semi-empirical methods have been reported to approach vibrational frequencies of organic molecules to within 10.4% (Healy and Holder 1993) or 9% (Holder and Dennington 1997). The greater magnitude of the errors observed when modeling these metal hydroxides may be traced to poorly defined empirical parameters for atoms with larger atomic numbers (Fe, Mg, Al).

Description of the clusters modeled

The unit cell of a typical dioctahedral phyllosilicate such as muscovite has 84 atoms. The size of this cluster ruled out the use of ab initio quantum mechanical methods (HF or DFT) with the resources presently available to the authors. Therefore, a smaller cluster representative of the environment of the OH group in dioctahedral phyllosilicates was defined. Frequencies of the OH group in large systems have been successfully approximated by modeling small clusters of atoms (Kubicki et al. 1993, 1995; Sainz-Díaz et al. 2000).

TABLE 1. Comparison between experimental and modeled wavenumbers (in cm^{-1}) of the gas phase Al(OH), Mg(OH), and $Fe(OH)_2$ metal hydroxides

		HF/6-31G*	HF/TZV	DFT/DND	PM3(tm)	High-level HF	Experiment
Al(OH)	Bend	111	463	134	356	155 *	-
	Al-OH stretch	893	844	822	938	845 *	810.30 †, 895.00 ‡
	AlO-H stretch	4268	4261	3764	4135	4017 *	3790.00 †
Mg(OH)	Bend	141	504	377	1005	516 §	–
	Mg-OH stretch	797	783	709	1131	676 §	–
	MgO-H stretch	4285	4253	3782	3929	4012 §	3214.00 ll
$Fe(OH)_2$	Bend	400–489	417	466–524	1037–1086	–	–
	Fe-OH stretch	676–725	644–768	701–849	914–925	–	735.50 #
	FeO-H stretch	4088–4132	4158–4203	3706–3714	3663–3665	–	–

* Vacek et al. 1993.
† Hauge et al. 1980.
‡ Pilgrim et al. 1993.
§ Kong and Boyd 1996.
ll Bunker et al. 1995.
Kauffman et al. 1985.

This study begins with modeling, at the DFT/DND level of theory, the smallest significant molecular cluster allegedly responsible for the OH fundamental vibrations. This cluster, subsequently named Small Dimer (Fig. 1a), consists of two octahedral cations and two hydroxyl groups: $[MM'(OH)_2]$, where the two octahedral cations may be Al^{3+}, Mg^{2+}, Fe^{2+}, or Fe^{3+}, and M and M' may or may not be the same element. The following Small Dimers were modeled: $[Al_2(OH)_2]^{4+}$, $[Mg_2(OH)_2]^{2+}$, $[Fe_2(OH)_2]^{2+}$, $[Fe_2(OH)_2]^{4+}$, $[AlMg(OH)_2]^{3+}$, $[AlFe(OH)_2]^{3+}$, $[AlFe(OH)_2]^{4+}$, $[MgFe(OH)_2]^{2+}$, $[MgFe(OH)_2]^{3+}$, and $[FeFe(OH)_2]^{3+}$. Cartesian coordinates of the atoms included in this cluster were obtained from single crystal X-ray diffraction data of muscovite (Rothbauer 1971).

The Dimer cluster (Fig. 1b) evolved from the Small Dimer by adding water molecules coordinated to the MM' cations, to increase the surrounding electron-density. The following Dimers were modeled: $[Al_2(OH)_2(H_2O)_8]^{4+}$, $[AlMg(OH)_2(H_2O)_8]^{3+}$, $[Mg_2(OH)_2(H_2O)_8]^{2+}$, $[AlFe(OH)_2(H_2O)_8]^{3+}$, $[Fe_2(OH)_2(H_2O)_8]^{2+}$, $[Fe_2(OH)_2(H_2O)_8]^{3+}$, $[AlFe(OH)_2(H_2O)_8]^{4+}$, $[Fe_2(OH)_2(H_2O)_8]^{4+}$, $[MgFe(OH)_2(H_2O)_8]^{3+}$, and $[MgFe(OH)_2(H_2O)_8]^{2+}$.

The effect on the OH fundamentals of having electrically charged clusters was analyzed by comparing ν(OH) of neutral and close-to-neutral Dimers of the form $[MM'(OH)_6(H_2O)_4]$, (starting coordinates from Kubicki, personal communication), to ν(OH) of the equivalent Dimers of the form $[MM'(OH)_2(H_2O)_8]$. The results[1] showed a strong, significant linear correlation ($R^2 = 0.94$) between both data sets. We conclude that the charge of the clusters affects the absolute values of the OH frequencies consistently, and therefore the trend among the clusters is preserved.

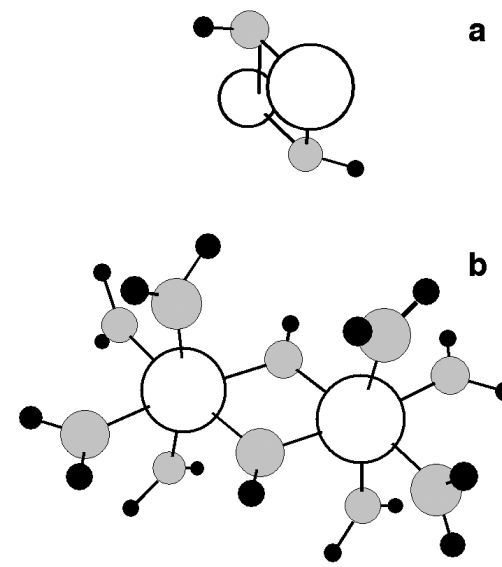

FIGURE 1. Starting structure of the Small Dimer (**a**) and Dimer (**b**) clusters. Open circles = octahedral cations; gray circles = O atoms, black circles = hydrogen atoms.

The spin state of Fe complexes

Theoretically derived crystal field splitting and electron pairing energies calculated for Fe^{2+} and Fe^{3+} in hexa-aqua environments (i.e., $[Fe(H_2O)_6]^{2,3+}$), indicate that the high-spin configuration is the most stable, since the electron pairing energies are larger than the crystal field splitting energies (Cotton and Wilkinson 1976). The same authors report experimental observations confirming this point. Also, ab initio calculations performed by Zwaans et al. (1996) on transition metal compounds (including Fe), confirm that high-spin configurations are the most stable. This is contrary to the approach taken by Sainz-Díaz and co-authors (2000), who considered Fe^{3+} in octahedral coordination to be in its low-spin configuration.

DFT calculations performed in this study for the Small Dimer $[MgFe(OH)_2]^{3+}$, with high and low-spin Fe, show that the high-spin configuration is the most stable, and that the spin configuration has a strong effect on the vibrational frequencies. The non-scaled calculated ν(OH) and δ(OH) wavenumbers are 2693 and 1160 cm^{-1}, respectively, for the low-spin configuration, and 2816 and 1111 cm^{-1} for the high-spin. Considering low-spin instead of high-spin produces differences in the calculated wavenumbers in the same order of magnitude as those caused by different octahedral cationic occupancy. In this study, Fe, both in its ferrous and ferric state, was considered to be in its high-spin configuration.

[1] $\nu[MM'(OH)_6(H_2O)_4]$ for MM' = (AlAl), (MgMg), and ($AlFe^{3+}$) are (3693, 3645), (3759, 3745) and (3596, 3595) cm^{-1}, respectively. $\nu[MM'(OH)_2(H_2O)_8]$ for the same cationic groups are (3638, 3633), (3744, 3735), and (3597, 3590, 3585, 3579) cm^{-1}, respectively.

Experimental IR data

IR transmittance spectra of 42 samples of muscovite, illite, and interlayered illite/smectite were acquired using a Nicolet Magna 760 FTIR (Fourier Transform Infrared) spectrophotometer, for analysis of OH-related fundamental modes of vibration. Despite differences in their crystal chemistry, layer charge, and vacant sites distribution, the OH groups in muscovite, illite, smectites, and other dioctahedral phyllosilicates are situated in basically analogous local structural environments. Therefore, their δ(OH) and ν(OH) fundamentals are to a large extent comparable. The transmittance spectra of pellets consisting of finely grained sample in a dried KBr matrix were acquired between 10 000 and 650 cm^{-1}, accumulating 200 scans at 4 cm^{-1} spectral resolution. The spectral sampling interval was 1.93 cm^{-1}, and the wavenumber accuracy 0.1 cm^{-1}, approximately.

Geochemical compositions for 36 of these samples were compiled from the literature (Gaudette et al. 1964; Hower and Mowatt 1966; Lin and Clemency 1981; Eberl et al. 1987; Post 1988; Post and Austin 1993; Post personal communication). Their octahedral compositions (available on request) were then calculated from the major element analyses, following the procedure devised by Ross and Hendricks (1945), based on a formula unit with 11 O atoms. Because compositions had been obtained in most cases using X-ray fluorescence analysis, differentiation between Fe^{2+} and Fe^{3+} was not possible. In this situation it is common practice to consider all the iron in its oxidized state. According to their composition, the following octahedral cation groups are the most common in our samples: Al_2, AlMg, and $AlFe^{3+}$.

Experimental IR data of other phyllosilicate samples, encompassing a wider variety of octahedral compositions, were compiled from the literature (Farmer 1974; Besson and Drits 1997; Cuadros and Altaner 1998; Redhammer et al. 2000). Common octahedral cation groups in these samples are Al_2, AlMg, $AlFe^{3+}$, Mg_2, Fe^{3+}_2, and $MgFe^{3+}$. The range of octahedral compositions covered by some of the samples included in this study is represented in Figure 2.

Assignment of the OH fundamentals identified in our samples (Table 2) was performed using fingerprinting techniques and by comparison to previous band assignments from the literature. OH fundamentals occur in the limbs of very strong absorption bands, such as the Si-O-Si stretch and the H_2O stretch (Fig. 3). This results in apparent shifts in the location of the OH fundamental band centers. In this study, location of the true band centers of the δ(OH) fundamentals was done by visual inspection of continuum-removed spectra. The spectra were divided by the convex hull connecting the local minimum (970 cm^{-1}) and maximum (808 cm^{-1}) of the larger absorption band on which the OH fundamental was superimposed. Bands for the same cationic environment were found to occur in a very restricted margin of wave numbers, usually within ±2 cm^{-1} around the mean. The continuum removal technique proved to be insufficient for the analysis of the ν(OH) bands, due to their complexity. In this case, spectral decomposition was performed using the software DecompIR (Lanson, personal communication), following the procedure described in Besson and Drits (1997). The variability observed in the band position was slightly larger in this case (approximately ±4 cm^{-1} around the mean), similar to that reported by Besson and Drits (1997) (3 cm^{-1} around the mean in a total of 23 samples), and contrasting with data from Redhammer et al. (2000) (up to 11 cm^{-1} from the mean in 9 samples). As has been previously discussed in the literature, deconvolution results are not unique (Scheinost et al. 1999). In fact, the deconvolution results in this study were found to be slightly dependent on starting conditions.

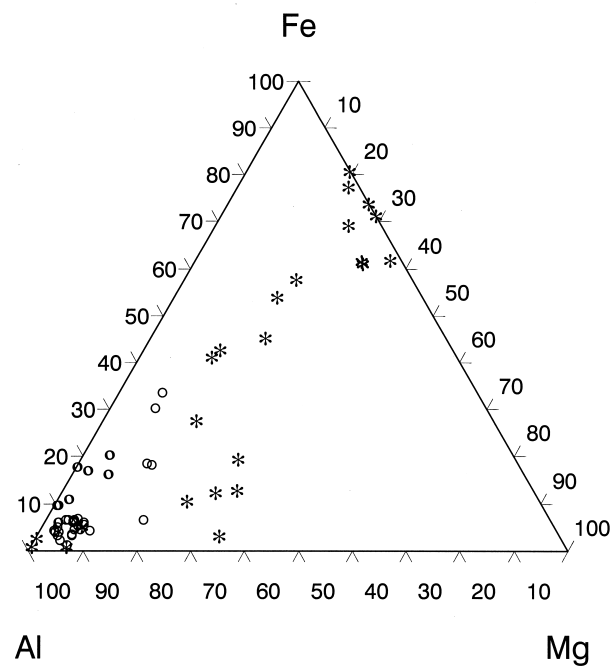

FIGURE 2. Octahedral cationic composition of some of the phyllosilicate samples included in this study. Circles correspond to illite and muscovite samples whose IR spectra were acquired as part of this study. Asterisks correspond to mineral data compiled by Besson and Drits (1997).

RESULTS AND DISCUSSION

IR bands assignment

The δ(OH) and ν(OH) fundamentals in the most common dioctahedral environments, as described in the literature, are shown in Figure 3. The most intense bands present in the OH bend region are two Si-O-Si asymmetric stretch bands (Salisbury et al. 1991) located at 1030–1090 cm^{-1}. Other Si-related bands in this region have been located at 796, 777, and 694 cm^{-1}. They correspond to Si-O-Si symmetric stretch modes (Salisbury et al. 1991). The fact that these features are present even in totally monomineralic samples, indicates that these bands may correspond to stretching motions in the tetrahedral sheet of the samples studied, although in some cases they may also be due to quartz impurities. Another band at 750 cm^{-1} appears consistently, even in samples with no accessory minerals. This band was interpreted as an Al-O-Si in plane-vibration by Farmer (1974) and by Cuadros and Altaner (1998).

In the 3615–3670 cm^{-1} range, several ν(Al_2OH) modes have been previously identified (Saksena 1964; Vedder 1964; Farmer

TABLE 2. Assignments of OH bands (in cm^{-1}) obtained in this study from visual inspection of continuum removed spectra [δ(MM'OH) modes], and from spectral deconvolution [ν(MM'OH) modes]

Sample	δ(MM'OH)				ν(MM'OH)				
	Al_2	Al_2	$AlFe^{3+}$	AlMg	Al_2	Al_2	Al_2	AlMg	Mg_2
BVC96001_1	(939)	916	875.5	829	3664	3639	3620	–	3583
BVC96002	–	914	877	–	–	–	3627	–	–
CHP94006	(939)	912	(875)	829	–	3637	3623	–	–
CHV96001_1	(935)	912	–	827	3650	–	3622	–	–
Guatemala	(931)	906	(879)	823	–	3639	3616	–	3589
Ruby	(931)	910	(875.5)	831	3652 3664	3643	3631 3620	3610	–
M. Gulch	(929.5)	914	(879)	827	3656	3643	3627	3612	3593
Tanzania	–	910	879	825	3653	3637	3624	3606	3591
Isinglass	(939)	914	879	829	3658	3649	3627	3602	–
Capitan	(929.5)	912	879	825	–	–	3626	–	3593
M. Alamo	(935)	914	879	829	3656	3645	3629 3618	–	3598
Pegma	–	(924)	(877)	829	3655 3665	3640	3626	3610	–
Empire	(935)	(914)	(877)	829	3662	3649 3635	3623	–	–
Miller-Walters I	(935)	912	(875)	829	3662	3647	3623	3604	–
Tip Top	(933)	914	875.5	829	3664 3650	–	3627	–	–
LCHP-E21-CH20	(933)	912	(875.5)	829	3662	3633	3622	–	–
LCHP-E66-ST1	(933)	912	(875.5)	829	3658	–	3631 3614	–	–
LCR017_3	(939)	(916)	(877)	829	–	–	3631 3622	–	–
SG4_3	939	914	(877)	837	3654	–	3626	–	–
AR1	(937–933)	910	–	829	3654	–	3629	3610	–
Miller-Walters II	(933)	916	(875)	829	3662	–	3627	3612	–
Miller-Walters III	(933)	912	(875)	829	3662	3647	3626	3606	–
Phillips	(933)	914	(875)	829	3666 3656	3643	3631 3618	–	–
Occidental	935	912	(875–872)	829	–	–	3631	–	–
IMT-1	–	910	875.5	829	3660	3645	3629	3608	3587
LF7	(933)	914	875.5	829	3653	–	3626	–	3570
RM11	(933)	916	873	829	3662	3647	3625	–	3579
RM21	(935)	914	875.5	829	3658	3645	3631 3620	3604	3571
RM22	(937)	916	873.6	829	3658	–	3627	–	3568
RM3	–	910	(875.5)	829	–	3645	3627	3610	3579
RM30	(935)	914	(875.5)	829	3668 3658	3645	3622	–	–
RM31	(935)	912	(877)	827	–	3649	3622	–	–
RM35A	(937)	914	877	829	3658	3643	3624	–	3573
RM4	(935)	912	879	829	–	–	3627	–	–
RM6	(937–933)	914	(877)	829	–	–	3626	–	3567
RM8	(933)	916	(875.5)	827	3658	3645 3635	3622	3606	3581
Fithian	–	912	875.5	(829)	3656	3647 3635	3620	3600	3583
Marblehead	–	912	879	834	–	–	3649 3631	3610 3604	3583
RM35C	(935)	914	875.5	829	3653	–	3626	–	–
RM35D	(935)	914	876	829	3653	–	3629	3612	–
SG1	(933)	914	877	831	3653	–	3629	–	–
Silverhill	–	911	875.5	829	–	–	3627	–	–
Average	935	913	876	829	3657	3643	3625	3607	3581
Std. Deviation	2.6	2.7	1.6	2.1	3.9	4.4	3.2	3.8	9.5

Note: Location of less defined bands are shown in parenthesis.

1974; Slonimskaya et al. 1986; Besson and Drits 1997). Saksena (1964) proposed OH located in different crystallographic sites of the unit cell and lack of perfect crystallinity as the causes for multiple ν(Al_2OH) bands in muscovite. Three of these bands are commonly present in the deconvolution results of our samples at 3625, 3643, and 3657 cm^{-1}, in agreement with assignments by Besson and Drits (1997) at 3621, 3641, and 3658 cm^{-1}.

In spectra of our samples containing octahedral Mg, bands at 3607 and 3582 cm^{-1} occur. Besson and Drits (1997) assigned these bands to ν(AlMgOH) (3604 cm^{-1}) and ν(Mg_2OH) (3583 cm^{-1}), respectively.

Spectral decomposition of our samples containing octahedral Fe, show a broad and less distinct ν(OH) band occurring near 3550 cm^{-1}. Because of its lack of definition, we could not locate this band satisfactorily. There is no general agreement in the assignments of Fe-related ν(OH) bands in the literature. Besson and Drits (1997) proposed the following sequence of wavenumbers: 3559 (Fe^{2+}Al), 3573 (Fe^{3+}Al), 3505 ($Fe^{2+}Fe^{3+}$), and 3535 cm^{-1} (Fe_2^{3+}). Redhammer et al. (2000) gave another interpretation for synthetic trioctahedral micas with octahedral

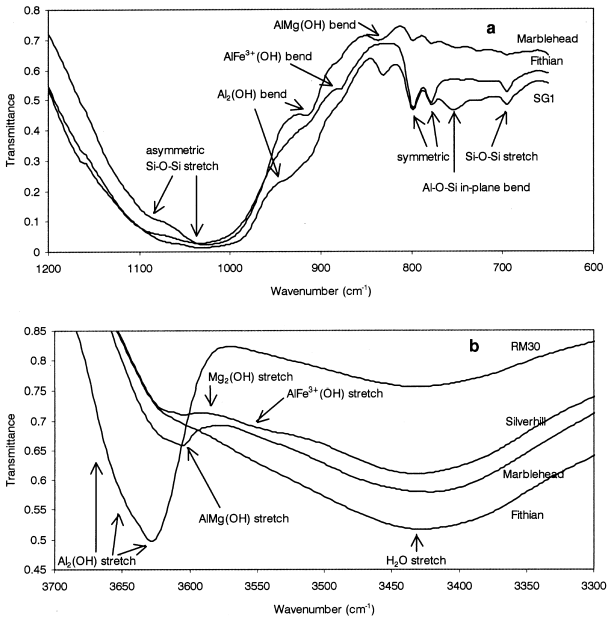

FIGURE 3. FTIR spectra of selected illite samples showing δ(OH) (**a**), ν(OH) (**b**), as well as other fundamentals, as assigned in the literature.

vacancies: 3600 ($Fe^{2+}Al$), 3579 ($Fe^{3+}Al$), 3542 ($Fe^{2+}Fe^{3+}$), and 3521 cm^{-1} (Fe^{3+}_2).

The ν(OH) bands described so far have been identified by Besson and Drits (1997) as corresponding to OH in mica-like local environments, that is, environments with a layer charge due to octahedral and/or tetrahedral cationic substitutions. ν(OH) bands in pyrophyllite-like local environments (without layer charge due to lack of octahedral and/or tetrahedral substitutions) have been also described (Besson et al. 1987; Petit et al. 1995; Besson and Drits 1997). According to Besson and Drits (1997), pyrophyllite-like Al_2, $AlFe^{3+}$, and Fe^{3+}_2 ν(OH) bands occur at 3675, 3652, and 3631 cm^{-1}, respectively. No pyrophyllite-like bands have been identified in our samples.

A well-developed band at 913 cm^{-1} is present in all our samples, as well as a less-developed band at 935 cm^{-1}, regardless of octahedral composition. We assign them to δ(Al_2OH) modes, in agreement with Farmer (1974), who found this mode in the 915–950 cm^{-1} range in all dioctahedral species. Petit (personal communication) assigned δ(Al_2OH) bands with larger δ wavenumbers (near 940 cm^{-1}) to species with mainly tetrahedral charge (e.g., beidellite, muscovite), and bands near 920 cm^{-1} to species with predominant octahedral charge (e.g., montmorillonite, phengite).

Finally, we assign the band located at 829 cm^{-1} in our samples to the δ(AlMgOH) mode, and the band located at 876 cm^{-1} to the δ($AlFe^{3+}OH$) mode. Farmer (1974) identified these bands at 840 and 890 cm^{-1} respectively in both celadonites and montmorillonites. Cuadros and Altaner (1998) distinguished between a ν(AlMgOH) mode at 820 cm^{-1} in illite and muscovite and another ν(AlMgOH) mode at 845 cm^{-1} in smectites.

The assignments of experimental frequencies proposed in this study, as well as assignments compiled from the literature, are summarized in Table 3.

Scaling of the frequencies modeled

Non-scaled vibrational frequencies calculated at the DFT/DND level of theory for ν(OH) and δ(OH) in different dioctahedral environments are listed in Table 4.

Ab initio harmonic vibrational frequencies are typically larger than the fundamentals observed experimentally (Hehre et al. 1986). The major sources for this disagreement are the neglect of anharmonicity effects in the theoretical treatment, incomplete incorporation of electron correlation, and the use of finite basis sets (Scott and Radom 1996).

Scott and Radom (1996) proposed computational method-dependent scaling factors suitable for frequency scaling. These scaling factors are independent of the vibrational modes and molecules considered. The most successful computational methods require scaling factors close to one.

Another approach to frequency scaling consists of using different scaling factors for different vibrational modes (Grunenberg and Herges 1997). According to these authors, the same scaling factor will not apply to all types of vibration. If electron correlation is not adequately considered, force constants theoretically derived may be overestimated, and more importantly, this will not be a systematic effect, but will depend on the nature of the bond. This technique requires the analysis of a set of molecules with similar bonds, and, there-

TABLE 3. Experimental wavenumbers (in cm^{-1}) of OH in phyllosilicates

Octahedral Composition	ν(OH)	δ(OH)
Al_2	3621*, 3641*, 3658 *, 3675 †, 3625 ll, 3643 ll, 3657 ll	915 ‡, 950 ‡, 915 §, 913 ll, 935 ll
Al Mg	3604 *, 3607 ll	840 ‡, 820 §, 845 §, 829 ll
Mg_2	3583 *, 3581 ll	–
$AlFe^{3+}$	3573 *, 3652 †, 3579 #	890 ‡, 875 §, 876 ll
Al Fe^{2+}	3559 *, 3600 #	–
Mg Fe^{3+}	3559 *	800 ‡, 780 §
Mg Fe^{2+}	3543 *	–
Fe^{3+}_2	3535 *, 3521 #, 3631 †	818 ‡, 797 §
Fe^{2+} Fe^{3+}	3521 *, 3542 #	800 ‡
Fe^{2+}_2	3505 *	–

* Besson and Drits (1997) on muscovite-like dioctahedral phyllosilicates.
† Besson and Drits (1997) on pyrophyllite-like dioctahedral phyllosilicates.
‡ Farmer (1974) on dioctahedral phyllosilicates.
§ Cuadros and Altaner (1998) on dioctahedral phyllosilicates.
ll this study on dioctahedral phyllosilicates.
Redhammer et al. (2000) on synthetic trioctahedral micas with octahedral vacancies.

TABLE 4. Non-scaled wavenumbers (in cm^{-1}) calculated at the DFT/DND level of theory for OH in various dioctahedral environments

Dioctahedral Environment	Small Dimers δ(OH)	Dimers δ(OH)	Small Dimers ν(OH)	Dimers ν(OH)
Al_2	1182	1069	2914	3638
Al Fe^{3+}	1111	954	2816	3597
Al Mg	1058	914	3337	3734
Fe^{3+}_2	1047	1007	2716	3518
Fe^{3+} Mg	993	968	3216	3648
Mg_2	947	872	3641	3744
$Fe^{2+}Fe^{3+}$	1011	942	3094	3595
Al Fe^{2+}	1029	980	3244	3691
Fe^{2+}_2	839	846	3418	3607
Mg Fe^{2+}	931	946	3543	3684

fore, similar vibration modes. Then each vibration mode is studied across the set of molecules, compared to experimental frequencies, and a vibration-specific scaling factor is derived.

Examination of plots showing experimental and modeled data (Fig. 4) indicates that a linear regression can fit both sets better than a scaling factor alone. This way it is possible to account for slope and offset differences between modeling results and experimental data. In this study, to scale the wavenumbers modeled, we applied a linear transformation calculated by linear regression between the modeled and experimental data. Calculated δ(OH) wavenumbers were scaled respect to the experimental frequencies published by Farmer (1974). The ν(OH) wavenumbers were scaled by comparison to experimental frequencies published by Besson and Drits (1997) for pyrophyllite-like environments, since these, like our clusters, are not affected by tetrahedral substitutions. The parameters of these linear transformations and R^2 values can be found in Table 5.

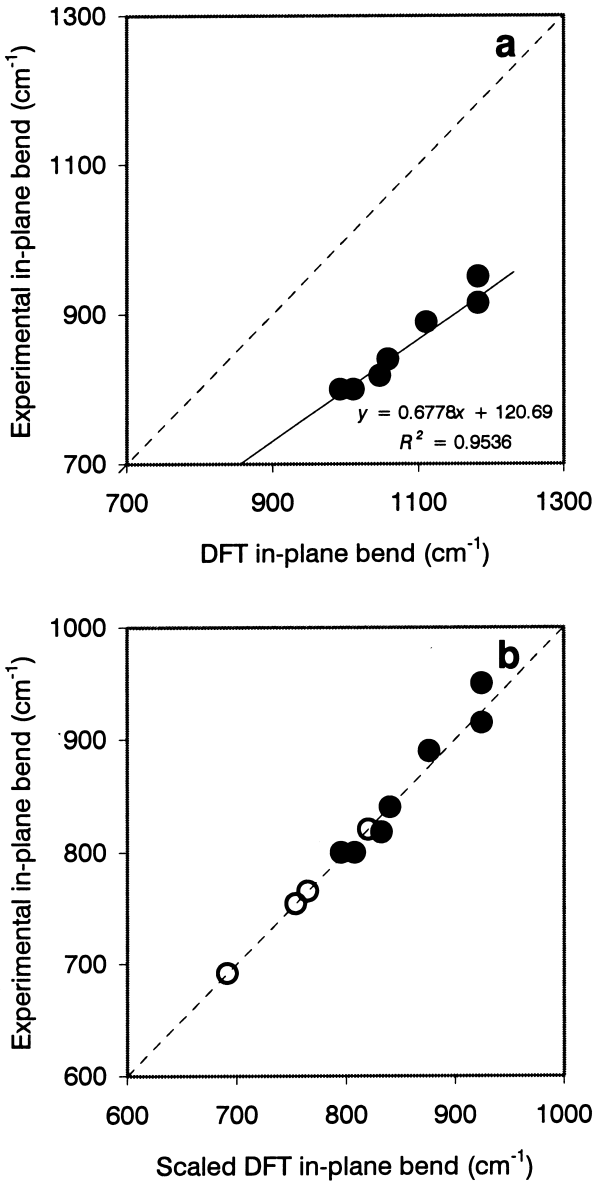

FIGURE 4. Experimental δ(OH) vibrational wavenumbers (compiled from Farmer 1974, numerical values shown in Table 3) vs. (**a**) non-scaled and (**b**) scaled wavenumbers calculated for the Small Dimer models. Hollow circles correspond to δ(OH) fundamentals in octahedral environments that have not previously been described in the literature.

Comparison between modeling results and experimental data

Scaled wavenumbers calculated in this study for the Small Dimer and Dimer clusters and experimental values corresponding to dioctahedral phyllosilicates of diverse octahedral composition are shown in Figure 5. Scaled wavenumbers calculated by Sainz-Díaz et al. (2000) at the HF-LANL2DZ level of theory are also included for reference.

The δ(OH) frequencies calculated in this study are in excellent agreement with experimental data reported by Farmer (1974) (Fig. 5a). The relative trend among experimental frequencies corresponding to different cationic environments of the OH is best preserved for the Small Dimers. The mean difference between scaled wavenumbers and experimental results is 8 cm^{-1} for the Small Dimers and 30 cm^{-1} for the Dimers. The differences between experimental and modeled wavenumbers for the Small Dimer clusters are the same order of magnitude as the differences between wavenumbers in different experimental sets (see Table 3), and could be explained by lack of exactness of the DFT functional used, errors introduced by the scaling, and variability in the mineral samples.

Certain δ(OH) frequencies that have not previously been identified experimentally in dioctahedral phyllosilicates were predicted by our calculations: 820 cm^{-1} for $AlFe^{2+}$, 691 cm^{-1} for Fe_2^{2+}, 754 cm^{-1} for $MgFe^{2+}$, and 765 cm^{-1} for Mg_2. The reasons why these frequencies have never been identified experimentally may be because octahedral occupancy by divalent cations is not common in dioctahedral phyllosilicates, and because other absorption bands, such as the symmetric Si-O-Si stretch, would mask these low-intensity bands.

We conclude that most of the variability observed in the δ(OH) frequencies of dioctahedral phyllosilicates can be explained by the nature of the neighboring octahedral cations alone. This finding confirms Farmer's (1974) and Sainz-Díaz et al.'s (2000) observations.

Figure 5b shows ν(OH) wavenumbers calculated in this study vs. experimental data for dioctahedral phyllosilicates published by Besson and Drits (1997). In this instance the wavenumbers calculated for the Dimer clusters are closer to experimental values than those calculated for the Small Dimers. The experimental ν(OH) data for muscovite-like environments and the modeling results for the Dimers follow parallel trends, but the experimental ν(OH) wavenumbers for mica-like envi-

TABLE 5. Parameters for the linear regressions $y = ax + b$ applied to scale the modeled wavenumbers, and R^2 values

OH vibration	Cluster	*a*	*b*	R^2
δ(OH)	Small Dimers	0.6778	120.69	0.9536
δ(OH)	Dimers	0.4539	400.94	0.2675
ν(OH)	Small Dimers	0.2222	3027.2	0.999
ν(OH)	Dimers	0.3531	2387	0.9577

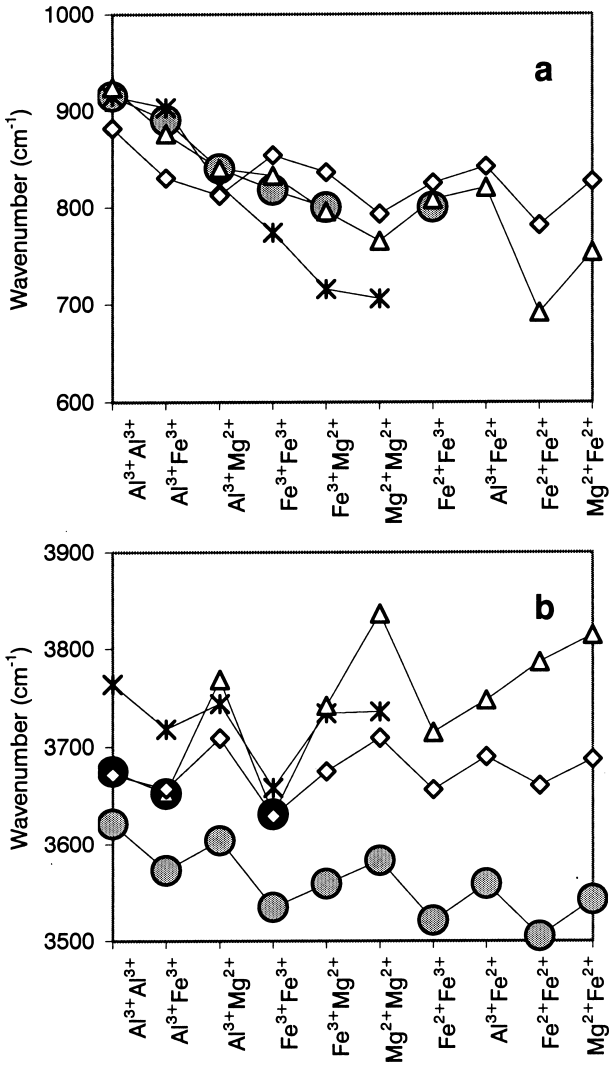

FIGURE 5. Wavenumbers corresponding to δ(MM'OH) (**a**), and ν(MM'OH) (**b**). Grey circles are experimental data (bend: Farmer 1974, stretch in muscovite-like environments: Besson and Drits 1997). Black circles are experimental data corresponding to pyrophyllite-like environments (Besson and Drits 1997). Triangles and diamonds are scaled wavenumbers calculated in this study for the Small Dimers and Dimers clusters, respectively. Asterisks are wavenumbers modeled and scaled by Sainz-Díaz et al. (2000).

ronments are consistently smaller than those predicted for pyrophyllite-like environments. The offset between them indicates the existence of other factors, besides the nature of the octahedral cations, governing the ν(OH) frequencies in dioctahedral environments. Negative charges due to cationic substitutions in the tetrahedral sheet could produce this offset, by making the OH bond grow longer and weaker, and consequently lowering its stretching frequency. The effect of charge (due to tetrahedral substitution) on the ν(OH) is substantial, and can be estimated to be on the order of 50 to 150 cm^{-1}.

ACKNOWLEDGMENTS

S.M.A. thanks the following institutions for their financial support: the Department of Geological Sciences and the Graduate School at CU Boulder, AAUW, GSA, CMS, AFMS, and CIRES. S.M.A. and J.R.R. also acknowledge support from the W. R. Wiley Environmental Molecular Sciences Laboratory. Thanks to B. Lanson for making his spectral decomposition software available for this study, and to D. Eberl, G. Swayze, and J. Post for interesting discussions and for facilitating access to their mineral collections. Thanks also to G. Swayze for introducing S.M.A. to FTIR spectra acquisition. We thank M.F. Brigatti, S. Petit, R. Frost, and an anonymous reviewer for their helpful comments. FTIR spectra were acquired in the USGS Spectroscopy Laboratory in Denver. Basis set 6-31G* for Fe was obtained from the Extensible Computational Chemistry Environment Basis Set Database, Version 1.0, as developed and distributed by the Molecular Science Computing Facility, EMSL, which is part of the PNNL, and funded by the U.S. DOE. The PNNL is a multi-program laboratory operated by Battelle Memorial Institute for the U.S. DOE under contract DE-AC06-76RLO 1830.

REFERENCES CITED

Becke, A.D. (1988) Density-functional exchange-energy approximation with correct asymptotic-behavior. Physical Review A, 38, 3098–3100.

———(1993) Density-functional thermochemistry. 3. The role of exact exchange. Journal of Chemical Physics, 98, 5648–5652.

Besson, G. and Drits, V.A. (1997) Refined relationships between chemical composition of dioctahedral fine-grained mica minerals and their infrared spectra within the OH stretching region. Part I: identification of the OH stretching bands. Clays and Clay Minerals, 45, 58–169.

Besson, G., Drits, V.A., Daynyak, L.G., and Smoliar, B.B. (1987) Analysis of cation distribution in dioctahedral micaceous minerals on the basis of IR spectroscopy data. Clay Minerals, 22, 465–478.

Beutelspacher, H. (1956) Agricultural research. Special edition, 7, 74–79 (in German) (not seen; extracted from The American Mineralogist, 49, 736, 1964).

Bunker, P.R., Kolbuszewski, M., Jensen P., Brumm, M., Anderson, M.A., Barclay, W.L., Ziurys, L.M., Ni, Y., and Harris, D.O. (1995) New rovibrational data for MgOH and MgOD and the internuclear potential function of the ground electronic state. Chemical Physics Letters, 239, 217–222.

Clark, R.N., King, T.V.V., Klejwa, M., and Swayze, G.A. (1990) High spectral resolution reflectance spectroscopy of minerals. Journal of Geophysical Research, 95, 12,653–12,680.

Clark, T., Chandrasekhar, J., Spitznagel, G.W., and Schleyer, P. von R. (1983) Efficient diffuse function-augmented basis-sets for anion calculations. 3. The 3-21 +G basis set for first-row elements, Li-F. Journal of Computational Chemistry, 4, 294–301.

Cotton, F.A. and Wilkinson, G. (1976) Basic inorganic chemistry, 579 p. Wiley, New York.

Cuadros, J. and Altaner, S.P. (1998) Compositional and structural features of the octahedral sheet in mixed-layer illite/smectite from bentonites. European Journal of Mineralogy, 10, 111–124.

Duke, E.F. (1994) Near infrared spectra of muscovite, Tschermak substitution, and metamorphic reaction progress: Implications for remote sensing. Geology, 22, 621–624.

Dunning, T.H. (1971) Gaussian basis functions for use in molecular calculations. III. Contraction of (10s6p) atomic basis sets for the first-row atoms. Journal of Chemical Physics, 55, 716.

Eberl, D.D., Środoń, J., Lee, M., Nadeaus, P.H., and Northtrop, H.R. (1987) Sericite from the Silverton Caldera, Colorado: Correlation among structure, composition, origin, and particle thickness. American Mineralogist, 72, 914–934.

Farmer, V.C. (1974) The layer silicates. In V.C. Farmer, Ed.,The Infrared Spectra of Minerals. Mineralogical Society Monograph 4, p. 331–363, London.

Fock, V. (1930) Approximation method for the solution of the quantum mechanical multi-body problem. Journal of Physics, 6, 126–148 (in German).

Francl, M.M., Pietro, W.J., Hehre, W.J., Binkley, J.S., Gordon, M.S., DeFrees, D.J., and Pople, J.A. (1982) Self-consistent molecular-orbital methods. 23. A polarization-type basis set for second-row elements. Journal of Chemical Physics, 77, 3654–3665.

Fripiat, J.J. (1960) Application of infrared spectroscopy to the study of clay minerals. Bulletin Groupe Français Argiles, 12, 25–41.

Gaudette, H.E., Eades, J.L., and Grim, R.E. (1964) The nature of illite. In W.F. Bradley and S.W. Bailey, Eds., Proceedings Thirteenth National Conference on Clays and Clay Minerals, October 5–8. p.33–48, Pergamon Press. The Clay Minerals Society. Madison, Wisconsin.

Grunenberg, J. and Herges, R. (1997) Calculation of molecular vibrations: selective scaling factors for semi-empirical force constants. Journal of Computational Chemistry, 18, 2050–2059.

Hartree, D.R. (1928a) The wave mechanics of an atom with a non-coulomb central field. Part I. Theory and methods. Proceedings Cambridge Philosophical Society, 24, 89–110.

———(1928b) The wave mechanics of an atom with a non-coulomb central field.

Part II. Some results and discussion. Proceedings Cambridge Philosophical Society, 24, 111–132.
Hauge, R.H., Kauffman, J.W., and Margrave, J.L. (1980) Infrared matrix-isolation studies of the interactions and reactions of group 3A metal atoms with water. Journal of the American Chemical Society, 102, 6005–6011.
Head-Gordon, M. (1996) Quantum chemistry and molecular processes. Journal of Physical Chemistry, 100, 13213–13225.
Healy, E.F. and Holder, A. (1993) An evaluation of AM1 calculated vibrational frequencies. Journal of Molecular Structure (Theochem), 281, 141–156.
Hehre, W.J., Ditchfield, R., and Pople, J.A. (1972) Self-consistent molecular orbital methods. XII. Further extensions of Gaussian-type basis sets for use in molecular orbital studies of organic molecules. Journal of Chemical Physics, 56, 2257–2261.
Hehre, W.J., Radom, L., Schleyer, P.vR., and Pople, J.A. (1986) Ab initio molecular orbital theory. Wiley, New York.
Hohenberg, P. and Kohn, W. (1964) Inhomogeneous electron gas. Physical Review, B136, 864–871.
Holder, A.J. and Dennington, R.D. (1997) An evaluation of SAM1 calculated vibrational frequencies. Journal of Molecular Structure (Theochem), 401, 207–218.
Hower, J. and Mowatt, T.C. (1966) The mineralogy of illites and mixed-layer illite/montmorillonites. American Mineralogist, 51, 825–854.
Jørgensen, P. (1964) Infrared absorption of O-H bonds in some micas and other phyllosilicates. Proceedings Thirteenth National Conference on Clays and Clay Minerals, 263–273.
Kauffman, J.W., Hauge, R.H., and Margrave, J.L. (1985) Studies of reaction of atomic and diatomic Cr, Mn, Fe, Co, Ni, Cu, and Zn with molecular water at 15 K. Journal of Physical Chemistry, 89, 3541–3547.
King, T.V.V. and Clark, R.N. (1989) Spectral characteristics of chlorites and Mg-serpentines using high-resolution reflectance spectroscopy. Journal of Geophysical Research, 94, 13,997–14,008.
Koch, W. and Holthausen, M.C. (2000) A chemist's guide to Density Functional Theory. Wiley-VCH, Weinheim.
Kohn, W. and Sham, L.J. (1965) Self-consistent equations including exchange and correlation effects. Physical Review A, 140, 1133–1138.
Kong, J. and Boyd, R.J. (1996) The $^2\Sigma^+$ states of HBeO, HMgO and HCaO. Journal of Chemical Physics, 104, 4055–4060.
Kubicki, J.D., Sykes, D., and Rossman, G.R. (1993) Calculated trends of OH infrared stretching vibrations with composition and structure in aluminosilicate molecules. Physics and Chemistry of Minerals, 20, 425–432.
Kubicki, J.D., Apitz, S.E., and Blake, G.A. (1995) G2 calculations on $[H_3SiO_4]^-$, $[H_4SiO_4]$, $[H_3AlO_4]^{2-}$, $[H_4AlO_4]^-$, $[H_5AlO_4]$: Basis set and electron correlation effects on molecular structures, atomic charges, infrared spectra, and potential energies. Physics and Chemistry of Minerals, 22, 481–488.
Lin, H.C. and Clemency, C.V. (1981) The kinetics of dissolution of muscovites at 25 °C and 1 atm CO_2 partial pressure. Geochimica et Cosmochimica Acta, 45. 571–576.
McLean, A.D. and Chandler, G.S. (1980) Contracted gaussian-basis sets for molecular calculations. 1. Second row atoms, z = 11–18. Journal of Chemical Physics, 72, 5639–5648.
Petit, S. Robert, J.L., Decarreau, A., Besson, G., Grauby, O., and Martin, F. (1995) Contribution of spectroscopic methods to 2:1 clay characterization. Bulletin des Centres de Recherches Exploration-Production ELF Aquitanie, 19, 119–147 (in French).
Petit, S., Madejová, J., Decarreau, A., and Martin, F. (1999) Characterization of octahedral substitutions in kaolinites using near infrared spectroscopy. Clays and Clay Minerals, 47, 103–108.
Pilgrim, J.S., Robbins, D.L., and Duncan, M.A. (1993) Photoionization electronic spectroscopy of AlOH. Chemical Physics Letters, 202, 203–208.
Post, J.L. (1988) Elemental analysis of mica resources in California. California Geology, 41, 3–13.
Post, J.L. and Austin, G.S. (1993) Geochemistry of micas from Precambrian rocks of Northern New Mexico. Circular 202, 20 p.
Post, J.L. and Noble, P.N. (1993) The near-infrared combination band frequencies of dioctahedral smectites, micas and illites. Clays and Clay Minerals, 41, 6, 639–644.
Rappe, A.K., Smedley, T.A., and Goddard, W.A. (1981) Flexible d basis sets for Sc through Cu. Journal of Physical Chemistry, 85, 2607–2611.
Rassolov, V.A., Pople, J.A., Ratner, M.A., and Windus, T.L. (1998) 6-31G* basis set for atoms K through Zn. Journal of Chemical Physics, 109, 1223–1229.
Redhammer, G.J., Beran, A., Schneider, J., Amthauer, G., and Lottermoser, W. (2000) Spectroscopic and structural properties of synthetic micas on the annite-siderophyllite binary: Synthesis, crystal structure refinement, Mössbauer, and infrared spectroscopy. American Mineralogist, 85, 449–465.
Ross, C.S. and Hendricks, S.B. (1945) Minerals of the montmorillonite group. U.S. Geological Survey Professional Paper, 205-B, 23–79.
Rothbauer, R. (1971) Investigation of a 2M-muscovite with neutron rays. New Yearbook of the Mineralogy Monthly Journal, 143–154 (in German).
Sainz-Díaz, C.I., Timón, V., Botella, V., and Hernández-Laguna, A. (2000) Isomorphous substitution effect on the vibration frequencies of hydroxil groups in molecular cluster models of the clay octahedral sheet. American Mineralogist, 85, 1038–1045.
Saksena, B.D. (1964) Infrared hydroxyl frequencies of muscovite, phlogopite and biotite micas in relation to their structures. Journal of the Chemical Society, Faraday Transactions, 60, 1715–1725.
Salisbury, J.W., Walter, L.S., Vergo, N., and D'Aria, D.M. (1991) Infrared (2.1–25 μm) spectra of minerals. The Johns Hopkins University Press, Baltimore.
Scheinost, A.C., Schulze, D.G., and Schwertmann, U. (1999) Diffuse Reflectance Spectra of Al Substituted Goethite: A Ligand Field Approach. Clays and Clay Minerals, 47, 156–164.
Schmidt, M.W. et al. (1993) General Atomic and Molecular Electronic Structure System. Journal of Computational Chemistry, 14, 1347–1363.
Scott A.P. and Radom, L. (1996) Harmonic vibrational frequencies: An evaluation of Hartree-Fock, Moller-Plesset, quadratic configuration interaction, Density Functional Theory, and semiempirical scale factors. Journal of Physical Chemistry, 100, 16502–16513.
Serratosa, J.M. and Bradley, W.F. (1958) Determination of the orientation of OH bond axes in layer silicates by infrared absorption. Journal of Physical Chemistry, 62, 1164–1167.
Slonimskaya, M.V., Besson, G., Dainyak, L.G., Tchoubar, C., and Drits, V.A. (1986) Interpretation of the IR spectra of celadonites and glauconites in the region of OH-stretching frequencies. Clay Minerals, 21, 377–388.
Stewart, J.P. (1988) Optimization of parameters for semiempirical methods. I. Method. Journal of Computational Chemistry, 10, 209–220.
Šťubičan, V. and Roy, R. (1961) Isomorphous substitution and infrared spectra of the layer lattice silicates. American Mineralogist, 46, 32–51.
Sutherland, G.B.B.M. (1955) Infrared and X-ray analysis of crystal structure. Nuovo Cimento Supplemento, II Serie, 10, 635–641.
Swayze, G.A. (1997) The hydrothermal and structural history of the Cuprite mining district, Southwestern Nevada: an integrated geological and geophysical approach, 341 p. Ph.D. dissertation, University of Colorado, Boulder.
Thiel, W. and Voityuk, A.A. (1992) Extension of the MNDO formalism to d-orbitals. Integral approximation and preliminary numerical results. Theoretica Chimica Acta, 81, 391–404.
Tsuboi, M. (1950) On the positions of the hydrogen atoms in the crystal structure of muscovite as revealed by the infrared absorption study. Bulletin of the Chemical Society of Japan, 3, 83–88.
Tuddenham, W.M. and Lyon, R.J.P. (1960) Infrared techniques in the identification and measurement of minerals. Analytical Chemistry, 3, 1630–1634.
Vacek, G., DeLeeuw, B.J., and Schaefer, H.F. (1993) The X AlOH-X HAlO isomerization potential energy hypersurface. Journal of Chemical Physics, 98, 8704–8709.
Vedder, W. (1964) Correlations between infrared spectrum and chemical composition of mica. The American Mineralogist, 49, 736–768.
Vedder, W. and McDonald, R.S. (1963) Vibrations of the OH ions in muscovite. Journal of Chemical Physics, 38, 1583–1590.
Yang, K., Browne, P.R.L., Huntington, J.F., and Walsheh, J.L. (2001) Characterising the hydrothermal alteration of the Broadlands-Ohaaki geothermal system, New Zealand, using short-wave infrared spectroscopy. Journal of Volcanology and Geothermal Research, 106, 53–65.
Zwaans, R., van Lenthe, J.H., and den Boer, D.H.W. (1996) Ab initio calculations on first-row transition metal porphyrins. 2. Ground state spin multiplicities, calculated ionisation potentials and electron affinities and their relation to catalytic activity. Teochem Journal of Molecular Structure, 367, 15–24.

MANUSCRIPT RECEIVED AUGUST 31, 2001
MANUSCRIPT ACCEPTED APRIL 24, 2002
MANUSCRIPT HANDLED BY MARIA FRANCA BRIGATTI